Mass-loss rates and dust-to-gas ratios for obscured Asymptotic Giant Branch stars of different metallicities[*]

Jacco Th. van Loon

Institute of Astronomy, Madingley Road, Cambridge CB3 0HA, United Kingdom

Abstract. The mass-loss rates and dust-to-gas ratios of obscured Asymptotic Giant Branch (AGB) stars are investigated for samples with different initial metallicities: in the Small and Large Magellanic Clouds (SMC & LMC) and in the Milky Way. The properties of their circumstellar envelopes can be explained in a consistent way if, both for obscured M-type AGB stars and for obscured carbon stars, the total (gas+dust) mass-loss rate $\dot{M}$ depends only weakly on initial metallicity whilst the dust-to-gas ratio ψ depends approximately linearly on initial metallicity.

1. Introduction

Asymptotic Giant Branch (AGB) stars develop strong mass loss at rates up to $\dot{M} \sim 10^{-5}$ M$_\odot$ yr^{-1} or more. The optical light of AGB stars with the highest $\dot{M}$ is almost entirely absorbed by their dusty circumstellar envelopes (CSEs), and re-emitted at longer wavelengths. These obscured AGB stars become very bright infrared (IR) objects, outshining any other star in a galaxy except for a few red supergiants (RSGs). During a brief period in their lives, they loose 50 to 80% of their initial mass. This makes them important contributors to the chemical enrichment of the interstellar medium (ISM) — they are possibly the main sources of dust particles in the Universe.

Individual galaxies differ in their metal content as a result of different star formation histories. For instance, two of our nearest neighbours, the Large and Small Magellanic Clouds (LMC & SMC) have current metallicities a factor ~ 2 and ~ 5 less than the average metallicity in the Milky Way ($\sim$solar). When pursuing a quantitative description of the history of star formation and chemical enrichment within a galaxy, it is essential to correctly take into account the mass loss from AGB stars and RSGs. This requires the dust-to-gas ratios in their CSEs to be known.

The paper is organised as follows: in Sect. 2 formulae are derived for deriving mass-loss rates and dust-to-gas ratios from measurements of optical depths and either luminosities or expansion velocities. Sect. 3 introduces samples of obscured AGB stars in the MCs and in the Milky Way and addresses the near-IR colours of their circumstellar envelopes. Relative mass-loss rates and dust-to-gas ratios are determined in Sect. 4 for the magellanic and galactic circumstellar envelopes around obscured AGB stars, and the results are discussed in Sect. 5. In Appendix A new identifications of mass-losing AGB stars with IRAS point sources in the LMC are presented and in Appendix B expansion velocities are discussed.

2. Formulae for dust-driven winds

The optical depth τ is proportional to the column density and dust-to-gas mass ratio ψ. The column density is proportional to the total mass density ρ and inner radius R_i of the dusty CSE. The dust grains in the dust-formation zone are assumed to be in radiative equilibrium with the incident stellar radiation field, keeping the effective temperature $T_{\rm eff}$ and the dust condensation temperature $T_{\rm d}$ fixed. Then $R_i^2 \propto L$, the stellar luminosity. The continuity equation yields $\dot{M} = 4\pi r^2 \rho v_{\rm exp}$, with gas+dust mass-loss rate $\dot{M}$, and expansion velocity $v_{\rm exp}$. Here the drift velocity — the velocity difference between the gas and dust fluids — is neglected, i.e. gas and dust are assumed to be well coupled (cf. Lamers & Cassinelli 1999). Gas pressure and wind-driving mechanisms other than radiation pressure on dust are neglected as well, although they become important for wind speeds below a few km s^{-1} (e.g. Steffen et al. 1997, 1998). It follows that the optical depth

$$\tau(\lambda) \propto \frac{\psi \dot{M}}{v_{\rm exp}\sqrt{L}} \tag{1}$$

The constant of proportionality includes a factor $\kappa(\lambda)$, the wavelength-dependent opacity of the dust, and a temperature dependence as $(T_{\rm d}/T_{\rm eff})^2$.

In a radiation-driven outflow the matter-momentum flux is coupled with the stellar photon-momentum flux via the momentum equation (Gail & Sedlmayr 1986)

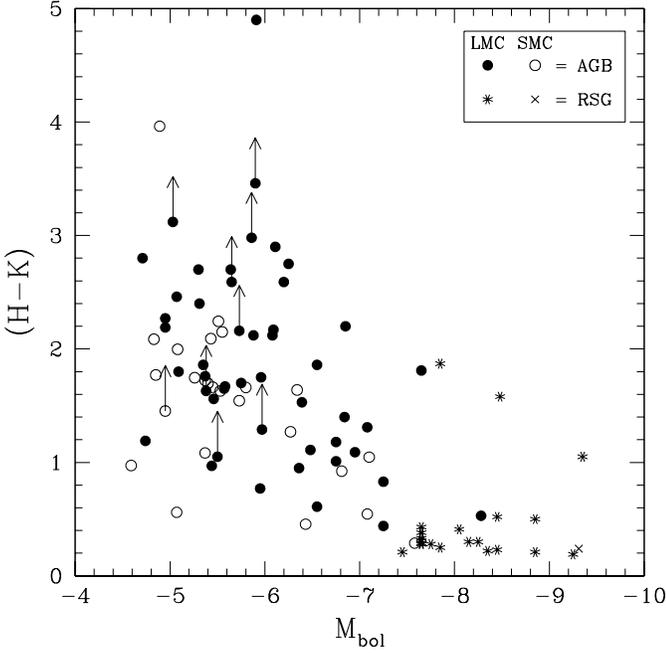$$\dot{M} v_{\rm exp} \propto \tau L \tag{2}$$

Fig. 1. $(H-K)$ colour versus bolometric magnitude for obscured AGB stars and red supergiants in the Magellanic Clouds. Colours are bluer for the more luminous stars.
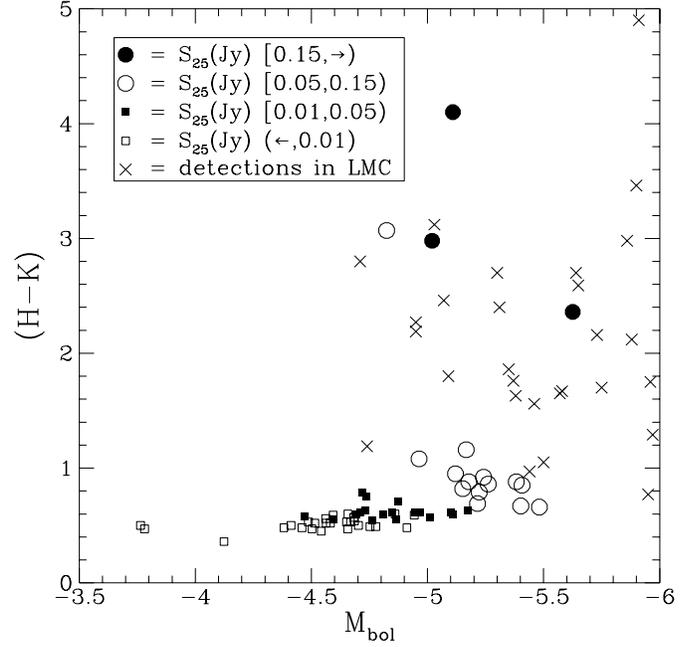
Fig. 2. $(H-K)$ colour versus bolometric magnitude for AGB stars in the South Galactic Cap (Whitelock et al. 1994). Different symbols are used according to the 25 μm flux density measured if the star were at the distance of the LMC. Crosses represent obscured AGB stars in the LMC (from Fig. 1).

with τ the flux-weighted optical depth. In general, the ratio of τ and $\tau(\lambda)$ depends on the mass-loss rate. Detailed computations such as those presented in Habing et al. (1994), however, show that this dependence vanishes for $\dot{M} > 10^{-5}$ $M_{\odot}$ yr^{-1}, which applies to the class of obscured AGB stars under study here (van Loon et al. 1999b). Combination of Eqs. (1) and (2) then leads to a description of the expansion velocity in terms of dust-to-gas ratio and luminosity:

$$v_{\exp} \propto \sqrt{\psi}\sqrt[4]{L} \qquad (3)$$

Eq. (2) can also be used to eliminate $v_{\exp}$ from Eq. (1), yielding a relation between the mass-loss rate and dust-to-gas ratio, and the optical depth and luminosity:

$$\log \dot{M} + 0.5 \log \psi + \text{constant} = \log \tau + 0.75 \log L \qquad (4)$$

Alternatively, Eq. (2) can be used to eliminate L from Eq. (1), yielding a relation between the mass-loss rate and dust-to-gas ratio, and the optical depth and expansion velocity:

$$\log \dot{M} + 2 \log \psi + \text{constant} = \log \tau + 3 \log v_{\exp} \qquad (5)$$

For magellanic stars luminosities are easier to measure than expansion velocities, and for these stars it is advantageous to make use of Eq. (4). For galactic stars the opposite is true, and for them Eq. (5) is the formula to use.

The constants in Eqs. (4) and (5) are related. Calling the constants of proportionality of Eqs. (1) and (2) respectively α and β, the constant in Eq. (4) equals $\log(\alpha/\beta)$ and the constant in Eq. (5) equals $\log(\alpha^2\beta)$. The constant of proportionality in Eq. (3) equals $\sqrt{\alpha\beta}$. The values of α and β depend on the properties of the dust species, and calibrating them is an important yet extremely difficult task that will not be exercised here.

3. Samples of obscured AGB stars

The optical depth scales with near-IR colours: $\tau \propto (H-K) - (H-K)_0$. The stellar photosphere is assumed to have $(H-K)_0 = 0.2$ mag. Fig. 3 in paper IV shows that galactic M-stars have $(H-K)_0 \sim 0.2$ mag, whilst galactic carbon stars may be slightly redder with $(H-K)_0 \sim 0.4$ mag. The sensitivity to the choice of $(H-K)_0$ rapidly vanishes as stars become obscured at $(H-K) \gtrsim 1$ mag.

Fig. 1 shows the $(H-K)$ colours of the obscured AGB stars and RSGs in the MCs (Loup et al. 1997; Zijlstra et al. 1996; van Loon et al. 1997, 1998a: papers I to IV). These samples are based on the identification of optical and near-IR counterparts of point sources detected at 12 and/or 25 μm by IRAS. The SMC photometry is mainly from Groenewegen & Blommaert (1998). Bolometric magnitudes for the SMC stars were determined in the same way as for the LMC stars by spline fitting to the spectro-photometric energy distribution (see Whitelock et al. 1994), adopting distance moduli of 18.55 and 18.97 mag for the LMC and SMC, respectively (Walker 1999). Also included are two newly identified obscured AGB stars in the LMC (Appendix A).

The reddest, optically thickest stars, with $(H-K) \gtrsim 3$ mag, are found among AGB stars with $M_{\rm bol} \sim -5$ to -6 mag. No such red objects are known in the MCs among the brightest AGB stars with $M_{\rm bol} \sim -7$ mag, nor amongst the RSGs. This is partly because bolometrically fainter stars have smaller inner radii of the dusty CSE and smaller expansion velocities, yielding larger τ (Eq. (1)) and redder $(H-K)$ colours at a given mass-loss rate.
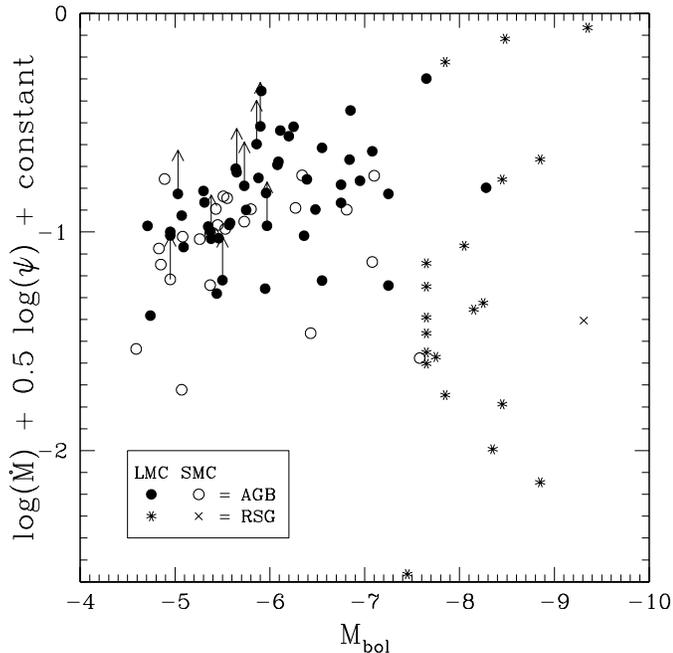
Fig. 3. Mass-loss rate $\dot{M}$ and dust-to-gas ratio ψ calculated from Eq. (4), versus $M_{\rm bol}$. There is a maximum to $\dot{M}$, increasing with higher luminosity. Mass-loss rates may be the same in SMC and LMC if ψ is sufficiently lower in the SMC.

Whitelock et al. (1994) have searched for Long Period Variables (LPVs) in the South Galactic Cap (SGC). Their sample consists of both optically bright and obscured AGB stars. Their $(H-K)$ colours are plotted versus bolometric luminosity in Fig. 2 (the Mira P-L relation was applied), where different symbols are used according to the 25 μm flux density measured if the star were at the distance of the LMC. The obscured stars that are detected by IRAS in the LMC have $S_{25} \gtrsim 0.1$ Jy. Their SGC equivalents have very red $(H-K)$ colours, though not redder than the reddest in the LMC (crosses). Optically bright AGB stars in the SGC sample have typically $(H-K) \sim 0.5$ and $M_{\rm bol} \sim -4$ to -5 mag. The MC samples do not contain such objects because their mid-IR emission is too faint to have been detected by IRAS at the distances of the MCs. On the other hand, the SGC sample is devoid of the brightest AGB stars with $M_{\rm bol} \sim -7$ mag as well as RSGs, because in the Milky Way such massive stars are preferentially found in the galactic plane.

There is a cluster of SGC stars with $(H-K) \sim 0.8$ and $M_{\rm bol} \sim -5.2$ mag (Fig. 2). These stars clearly show circumstellar reddening, but the mid-IR emission from their CSEs is just below the detection limit of IRAS when placed at the distance of the LMC. This leaves open the possibility of the existence in the LMC of a potentially large population of AGB stars with moderate mass-loss rates and luminosities. Indeed, in paper III several field stars were found that are not related to a nearby IRAS source but that nevertheless had near-IR colours indicative of reddening. Recent ISO observations confirm the presence of this AGB population (Loup et al. 1999).

Wood et al. (1998) find LPVs in the Galactic Centre with K-band magnitudes from 5 to 13 after correction for interstellar extinction. At the distance of the LMC this would yield K-band magnitudes from 9 to 17, i.e. within the sensitivity of the searches in papers II & III and in Groenewegen & Blommaert (1998). The interstellar extinction corrected $(H-K)$ colours of the Galactic Centre LPVs average ~ 2 mag and are ~ 4 mag maximum, similar to the $(H-K)$ colours of the obscured AGB stars in the LMC. Wood et al. argue that their sample includes stars with initial metallicities a few times solar, and Blommaert et al. (1998) indeed find very red objects with $(H-K) > 4$ mag as inferred from their K- and L-band photometry.

Groenewegen et al. (1998) observed and modelled obscured carbon stars in the Milky Way. They used the P-L relation for carbon Miras to infer distances to the individual stars, that are found to be typically within 2 kpc from the Sun. Their two most obscured carbon stars have $(H-K) = 5.5$ and 8.0 mag. They also compiled a sample of oxygen-rich stars with near-IR photometry, pulsation periods and expansion velocities, without overlap with the SGC and Galactic Centre samples. The most obscured of these M stars have $(H-K) \sim 6$ mag.

4. Relative mass-loss rates and dust-to-gas ratios

In determining mass-loss rates and dust-to-gas ratios in the MCs one can rely on the use of luminosities and eliminate $v_{\rm exp}$ from Eq. (1). Luminosities are difficult to measure for stars in the Milky Way, however, due to unknown distances and severe interstellar extinction. Often the Mira P-L relation is applied to infer distances to individual stars, but this relation possibly breaks down for stars whose stellar mantles have been significantly reduced due to mass loss (e.g. Blommaert et al. 1998; Wood et al. 1998; Wood 1998), or obscured AGB stars may fall on other, parallel sequences (Bedding & Zijlstra 1998; Wood 1999). For the Milky Way stars, L is eliminated from Eq. (1), leaving $v_{\rm exp}$ to be measured. Because $v_{\rm exp}$ has been measured for only a few LMC stars, Eq. (3) will be used for the remaining LMC stars to estimate $v_{\rm exp}$ from L (see Appendix B). Although these estimates are likely to be accurate within a few km s^{-1}, the contribution of the uncertainty in $v_{\rm exp}$ is enlarged by a factor three in Eq. (5).

Eqs. (4) & (5) are used here to compare the combination of mass-loss rate and dust-to-gas ratio between the MCs and between the LMC and the Milky Way, respectively. If the mass-loss rate depends on luminosity but not on initial metallicity and if the luminosity distributions of the stars in these samples are identical — implying identical star formation histories — then the distributions over the combination of $\dot{M}$ and ψ are identical except for possible offsets due to different mean values for ψ among the different samples. The stars within each of the samples are likely to cover a range in initial metallicities due to their different progenitor masses and hence different formation epochs. Similar star formation histories, however, are anticipated to result in similar distributions over initial metallicity, and it is therefore meaningful to assign a mean initial metallicity and a mean value for ψ to each of the samples.

Eq. (4) is used to calculate the combination of mass-loss rate and dust-to-gas ratio from the optical depths and lu-

Table 1. Mean and error in the mean of the values of ($\log \dot{M} + 0.5 \log \psi + \text{constant}$) for the distributions of obscured AGB stars in the LMC and SMC. Also the differences between the various (sub-)distributions are listed.

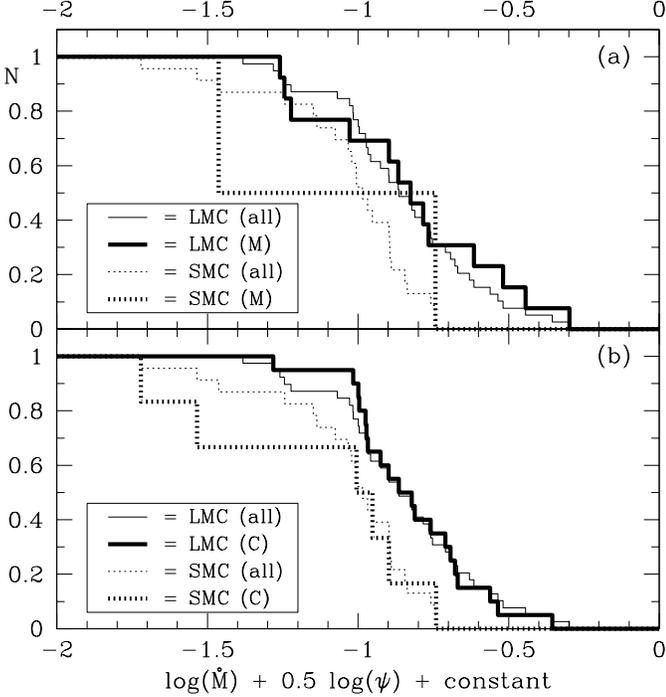|	[total]	[C]	[M]	[C] − [total]	[M] − [total]	[C] − [M]
[LMC]	-0.85 ± 0.04	-0.83 ± 0.05	-0.83 ± 0.09	0.02 ± 0.06	0.02 ± 0.09	0.00 ± 0.10
[SMC]	-1.04 ± 0.05	-1.14 ± 0.16	-1.10 ± 0.36	-0.10 ± 0.17	-0.06 ± 0.36	-0.04 ± 0.39
[LMC] − [SMC]	0.19 ± 0.07	0.32 ± 0.17	0.28 ± 0.37			

Fig. 4a and b. Normalised distribution of obscured AGB stars ($M_{\text{bol}} \gtrsim -7.5$ mag) over mass-loss rate $\dot{M}$ and dust-to-gas ratio ψ. Boldfaced are the sub-distributions of confirmed M-type stars **a** and confirmed carbon stars **b** amongst the obscured AGB stars.

Fig. 5. Mass-loss rate $\dot{M}$ and dust-to-gas ratio ψ calculated from Eq. (5), plotted versus pulsation period P for obscured AGB stars in the LMC (Wood et al. 1992; Wood 1998; van Loon et al. 1998b), South Galactic Cap (Whitelock et al. 1994), Galactic Centre (Wood et al. 1998) and "Solar neighbourhood" (Groenewegen et al. 1998). Dotted vertical lines delineate regimes of periods $P < 500$, $500 \leq P < 800$ and $P \geq 800$ d.

minosities for the magellanic stars (Fig. 3). The stars with $M_{\text{bol}} < -7.5$ and > -7.5 mag are considered to be RSGs and obscured AGB stars, respectively (see van Loon et al. 1999b), except for the well-studied luminous obscured AGB star IRAS05298−6957 ($M_{\text{bol}} = -7.65$ mag) and the weakly mass-losing RSG HV2700 ($M_{\text{bol}} = -7.45$ mag). IRAS04498−6842 ($M_{\text{bol}} = -8.28$ mag) was classified as an AGB star (paper II), but here it is re-classified as a RSG (see also paper IV). Fig. 4 shows the cumulative distributions (normalised to unity) of the obscured AGB stars in the LMC (solid) and SMC (dotted) over the value of ($\log \dot{M} + 0.5 \log \psi + \text{constant}$). These do not include the few stars that have lower limits to their $(H - K)$ colours. The distributions for the subsamples of spectroscopically confirmed carbon stars and oxygen-rich (M-type) stars (van Loon et al. 1999b, and references therein; Groenewegen & Blommaert 1998) are boldfaced in Figs. 4a and b, respectively. Despite the small numbers for some of the sub-distributions, especially the M-type stars in the SMC, the shapes of the cumulative distributions are very similar. Both in the LMC and
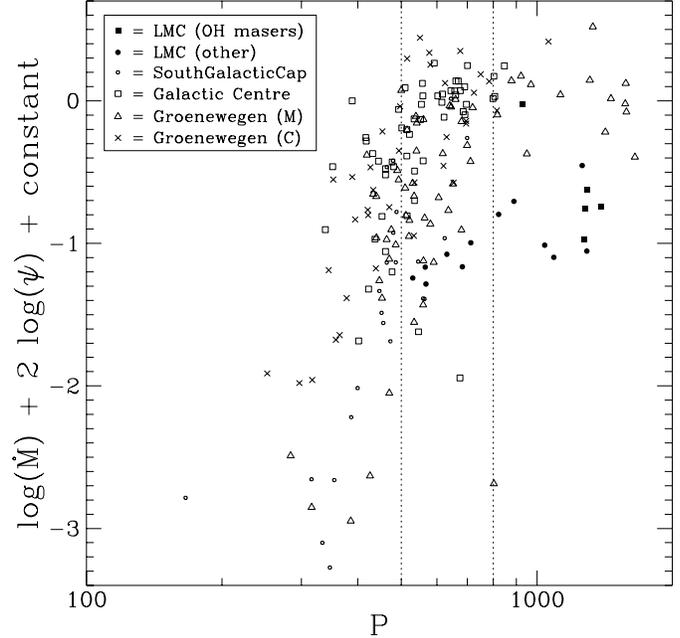
SMC the obscured M-type AGB stars and the obscured carbon stars have distributions that are coincident to a very high degree (Table 1). The only difference in the distributions is the systematic offset between those in the LMC compared to those in the SMC (Table 1). This offset is a 3σ result for the obscured AGB stars as a whole, a 2σ result for the obscured carbon stars, and consistent for the obscured M-type AGB stars (though not significant by itself).

Eq. (5) is used to calculate the combination of mass-loss rate and dust-to-gas ratio from the optical depths and expansion velocities for the obscured AGB stars in the LMC and the Milky Way (Fig. 5). Only LMC stars for which periods are known from the literature (Wood et al. 1992; Wood 1998) are plotted. Stars in the different samples are not similarly distributed over P, with the LMC sample having an average pulsation period longer than that of the Milky Way sample, possibly due to selection effects or differences in the star formation histories. Hence the populations of stars in these samples may not be directly compared.
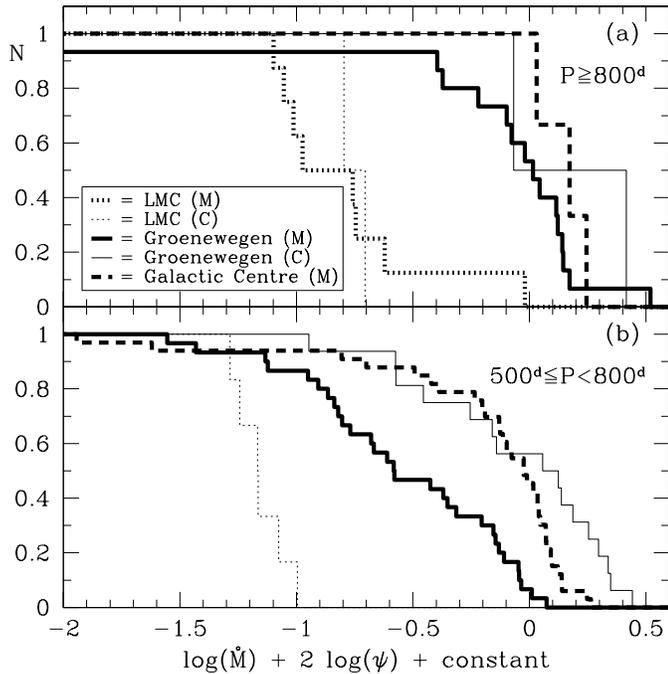
Fig. 6a and b Normalised distribution of obscured AGB stars in the LMC and in the Milky Way over mass-loss rate $\dot{M}$ and dust-to-gas ratio ψ for pulsation periods $P \geq 800$ d **a** and $500 \leq P < 800$ d **b**.

Table 2. Mean and error in the mean of the values of $(\log \dot{M} + 2\log\psi + \text{constant})$ for the distributions of obscured AGB stars in the LMC, in the Galactic Centre (GC), and in the "Solar neighbourhood" (Groen; excluding the point at $P = 802$ d and a value of -2.7). Also the differences between the various (sub-)distributions are listed.

	[C]	[M]	[C] − [M]
	$500 \leq P < 800$ d		
[LMC]	-1.16 ± 0.04		
[Groen]	-0.06 ± 0.10	-0.55 ± 0.08	0.49 ± 0.13
[GC]		-0.19 ± 0.08	
[Groen] − [LMC]	1.10 ± 0.11		
[GC] − [Groen]		0.37 ± 0.12	
	$P \geq 800$ d		
[LMC]	-0.75 ± 0.05	-0.79 ± 0.12	0.04 ± 0.13
[Groen]	0.17 ± 0.24	0.01 ± 0.06	0.17 ± 0.25
[GC]		0.15 ± 0.06	
[Groen] − [LMC]	0.93 ± 0.25	0.79 ± 0.14	
[GC] − [LMC]		0.93 ± 0.14	
[GC] − [Groen]		0.14 ± 0.09	

Two regimes of pulsation period will be focussed on: one for $500 \leq P < 800$ d, and another for $P \geq 800$ d. The first group consists of stars that evolve beyond the optically bright Mira phase with moderate $\dot{M}$ and into the obscured AGB phase (Jura 1986). The distribution of these stars in Fig. 5 suggests that they still increase in mass-loss rate and/or that they represent a large range in stellar masses. The second group consists of more evolved (or more massive) stars for which $\dot{M}$ has become so high that they shed their mantles on a timescale much shorter than the nuclear burning timescale. Hence these stars stay at constant luminosity while their pulsation periods keep increasing as their mantles are steadily diminished. The lack of any clear correlation between $\dot{M}$ and P in this part of Fig. 5 suggests that thereby the mass-loss rate remains essentially constant. Stars in the LMC sample are predominantly found in the second class of objects, whilst these kind of stars are very rare in the Galactic Centre sample due to their faintness in the K-band. M-type stars in the "Solar neighbourhood" sample of Groenewegen et al. (1998) populate both regimes rather evenly.

The relative distributions of mass-loss rates and dust-to-gas ratios are derived from Fig. 6 for the LMC (dotted), "Solar neighbourhood" (M-type; solid) and Galactic Centre (dashed), in the same way as before by estimating the relative offsets in $(\log \dot{M} + 2\log\psi + \text{constant})$ of the normalised cumulative distributions. The sample of obscured AGB stars with $500 \leq P < 800$ d in the "Solar neighbourhood" (Groenewegen et al. 1998) is clearly inhomogeneous: (i) the distribution of obscured M-type AGB stars is much flatter than all other distributions, indicating a wide range of stellar parameters, and (ii) the distribution of obscured carbon stars is offset with respect to the distribution of obscured M-type AGB stars — a 4σ result (Table 2). This may reflect differences in age (initial stellar mass) and/or initial metallicity, as the sub-samples of obscured M-type AGB stars and obscured carbon stars in the Groenewegen et al. sample have been selected in a very different way. The distributions of the obscured M-type AGB stars and obscured carbon stars in the LMC sample are, again, indistinguishable (Table 2). The Galactic Centre sample is positively offset with respect to both the Groenewegen et al. sample (3σ result for $500 \leq P < 800$ d) and the LMC sample (7σ result).

5. Discussion

5.1. Metallicities of obscured AGB stars in the Magellanic Clouds and in the Milky Way

What are the initial metallicities of the obscured AGB stars in the samples under study? First I discuss the dust-to-gas ratios in the ISM, before discussing metallicities of relatively young stellar populations. These considerations lead to estimates of the typical initial metallicities of the obscured AGB stars under study. These will then be used to correlate the mass-loss rates and dust-to-gas ratios with initial metallicity.

Most of the mass of stars that eventually evolve into AGB stars is returned to the ISM, enriched with dust. These intermediate-mass stars are sufficiently numerous and short-lived that the ISM has been recycled by them at least several times over the history of their parent galaxy. A 5 $M_\odot$ star has a lifetime of $\sim 1.1 \times 10^8$ yr (Marigo et al. 1999), and there have been already $\sim 10^2$ generations of these massive AGB stars at work in mixing dust with the ISM. Dust-to-gas ratios in the ISM of the LMC are found to be $\sim \frac{1}{4}$ of that of the ISM in the Solar neighbourhood (van Genderen 1970; Koornneef 1982; Clayton & Martin 1985), and in the SMC it is $\sim \frac{1}{10}$ of that in the Solar neighbourhood (van den Bergh 1968; van Genderen 1970; Lequeux et al. 1982; Bouchet et al. 1985). Dust is being
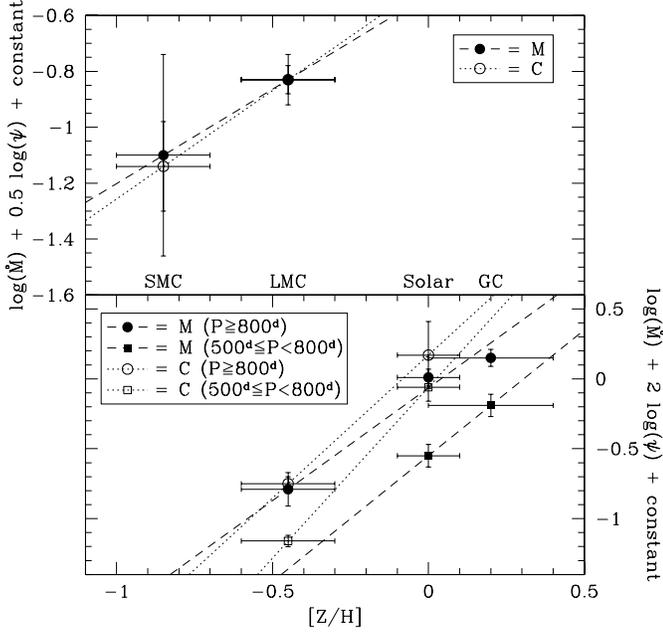
Fig. 7. Mass-loss rates and dust-to-gas ratios for the obscured AGB stars in the SMC, LMC, "Solar neighbourhood" and Galactic Centre, as a function of their initial metallicities.

destroyed in the ISM by shocks and gas accretion, especially in Star Formation Regions. Hence the dust-to-gas ratios in the ISM may only pose a lower limit to the dust-to-gas ratios in the CSEs of obscured AGB stars.

Initial metallicities for relatively young (10^{7-8} yr) field stars are found to be about 2 and 5 times lower in the LMC and SMC, respectively, compared to Solar metallicity (Spite et al. 1989a,b; Russell & Bessell 1989; Meliani et al. 1995; Luck et al. 1998). When depicting the chemical evolution of the MCs, however, it is clear that the initial metallicity with which stars were born a few Gyr ago was considerably lower — roughly twice — than what is measured in massive stars today (de Freitas Pacheco et al. 1998; Da Costa & Hatzidimitriou 1998; Bica et al. 1998). Obscured AGB stars, with a characteristic age of 10^9 yr, are thus expected to have initial metallicities somewhat lower than those measured in young field stars. Stars in the central regions of the Milky Way galaxy are found to cover a range in metallicity from sub- to super-solar, with the most easily observed obscured AGB population likely to comprise relatively massive stars of slightly super-solar initial metallicity (Rich 1988; Wood et al. 1998).

These considerations lead us to adopt a typical initial metallicity (logarithmic) of $[Z/H] = -0.85 \pm 0.15$ for obscured AGB stars in the SMC, $[Z/H] = -0.45 \pm 0.15$ in the LMC, $[Z/H] = 0.00 \pm 0.10$ in the Solar neighbourhood, and $[Z/H] = 0.20 \pm 0.20$ in the Galactic Centre. The margins are rough estimates for the typical range in initial metallicities, meaning that the typical metallicity for the sample is not expected to lie outside of these margins.

5.2. Mass-loss rates and dust-to-gas ratios

The values for the combination of mass-loss rates and dust-to-gas ratios as derived from using Eqs. (4) & (5) and listed in Tables 1 & 2 are plotted in Fig. 7. First order polynomials are drawn through the points. For the obscured M-type stars with $500 \leq P < 800$ d the polynomial was forced to cross the LMC data point, while the average was taken of the slopes obtained by either omitting the "Solar neighbourhood" data point or the Galactic Centre data point. The slopes of the polynomials can be used to constrain the dependence of the mass-loss rate on initial metallicity z (with $\log z = [Z/H]$) and the dependence of the dust-to-gas ratio on z, assuming that $\dot{M} \propto z^a$ and $\psi \propto z^b$. It then follows that the slope for $(\log \dot{M} + 0.5 \log \psi + \text{constant})$ equals $a + 0.5b$, and the slope for $(\log \dot{M} + 2 \log \psi + \text{constant})$ equals $a + 2b$. The sub-samples that had been selected according to the pulsation periods have, in fact, very similar slopes, and hence their averages are taken. Thus I find for the obscured M-type AGB stars that $a + 0.5b \sim 0.68$ and $a + 2b \sim 1.71$, whilst I find for the obscured carbon stars that $a + 0.5b \sim 0.78$ and $a + 2b \sim 2.24$. This yields for the dependences of the mass-loss rate and dust-to-gas ratio on initial metallicity for obscured AGB stars:

$$
\begin{aligned}
\log \dot{M}_{\mathrm{M}} &= 0.3^{+0.7}_{-1.3} & \log z + \text{constant} \\
\log \dot{M}_{\mathrm{C}} &= 0.3^{+0.6}_{-0.6} & \log z + \text{constant} \\
\log \psi_{\mathrm{M}} &= 0.7^{+0.6}_{-0.3} & \log z + \text{constant} \\
\log \psi_{\mathrm{C}} &= 1.0^{+0.3}_{-0.3} & \log z + \text{constant}
\end{aligned}
$$

The reader should realise that these exponents are indicative, but not very accurate. The errors (excluding those resulting from uncertainties in the adopted initial metallicities) mainly result from the small number of spectroscopically confirmed carbon and M-type stars in the SMC. If the initial metallicity dependence of the mass-loss rate and dust-to-gas ratio is really as similar as suggested here, then the obscured AGB stars in the SMC and LMC may be compared without distinction by chemical type, and the resulting errors on the exponents will become much smaller without significantly changing the values of the exponents themselves. Clearly, it is shown that the method employed here has the prospect of constraining the initial metallicity dependences of the mass-loss rate and dust-to-gas ratio for obscured AGB stars. Suitable data have only recently become available, and more such data are needed to improve on the preliminary results.

5.3. Obscured M-type AGB stars and carbon stars

Obscured M-type AGB stars and obscured carbon stars have been treated separately for two reasons: (i) the optical properties of their circumstellar dust are different, possibly leading to differences in the constants of proportionality α and β in Eqs. (1) and (2), respectively, and (ii) their dust-to-gas ratios and/or mass-loss rates may depend differently on initial metallicity. I here discuss these two issues in more detail.

Both α and β depend on the dust-type through the wavelength dependent opacity $\kappa(\lambda)$ and the flux-weighted opacity κ, respectively. Using Eq. (4) in the LMC yields indistinguishable distributions of the obscured M-type AGB stars and of the obscured carbon stars. However, in the LMC, obscured carbon stars are bolometrically fainter and exhibit lower mass-loss rates than obscured M-type AGB stars (van Loon et al. 1999b), which is expected to result in an offset between the distributions over $(\log \dot{M} + 0.5 \log \psi + \text{constant})$. The fact that this offset is not seen must mean that, by mere coincidence, the differences in $(\log \dot{M} + 0.5 \log \psi)$ are counteracted upon by the differences in $\kappa(\lambda)/\kappa$: at a given luminosity, dust-to-gas ratio and mass-loss rate, obscured carbon stars are redder than obscured M-type AGB stars. Also the coincidence between the distributions of obscured M-type AGB stars and obscured carbon stars using Eq. (5) in the LMC for $500 \leq P < 800$ d must be coincidental and/or due to low number statistics (only two obscured carbon stars), as the constant in Eq. (5) is proportional to $\kappa^2(\lambda)\kappa$ and differences in optical properties between the different dust species are likely to become apparent. This may explain at least partly the differences in distributions between the obscured M-type AGB stars and obscured carbon stars in the "Solar neighbourhood".

Obscured M-type AGB stars and obscured carbon stars seem to show very similar dependencies of their dust-to-gas ratios and especially their mass-loss rates on initial metallicity. There is no a-priori reason why the mass-loss mechanism should have a different dependency on initial metallicity for stars with different chemical types of circumstellar dust, other than due to a different dependency of their dust-to-gas ratios on initial metallicity. The similarity between the dependencies of the dust-to-gas ratio on initial metallicity is surprising. For obscured M-type AGB stars one may expect that the fraction of metals that are available for the formation of dust particles scales directly with the oxygen abundance in the photosphere, which scales at least approximately directly with the initial metallicity of the star. Hence a direct proportionality between dust-to-gas ratio and initial metallicity may not come as a surprise for obscured M-type AGB stars. For obscured carbon stars, however, the situation is very different: carbon stars only become carbon stars after 3rd dredge-up has enhanced the carbon abundance in the photosphere from $[C/O] < 1$ to $[C/O] > 1$. For obscured carbon stars it is crucial to know the photospheric abundances of both carbon and oxygen, because the carbon is locked into CO molecules until oxygen exhaustion and hence only the carbon excess is available for dust formation. It was thought that at lower initial metallicity, the lower oxygen abundance would make it easier for 3rd dredge-up to raise $[C/O]$ above unity, but the fact that no optically bright luminous carbon stars were found in the MCs meant that it is not that simple (Iben 1981). Not only is it poorly understood how 3rd dredge-up depends on initial metallicity (but see Marigo et al. 1999), there is also a second important phenomenon active: carbon star formation is avoided as long as the stellar mantle is massive enough to yield pressures and temperatures at the bottom of the convective layer sufficiently high for processing of carbon into oxygen and ni-

trogen to occur (Hot Bottom Burning; Iben & Renzini 1983; Wood et al. 1983). Thus it remains to be seen how the carbon excess for obscured carbon stars depends on initial metallicity (see also van Loon et al. 1999a). The data and analysis presented here suggest that the carbon excess for obscured carbon stars may be directly proportional to the initial metallicity.

6. Summary

In conclusion, the comparison between the dust-to-gas ratios and mass-loss rates of obscured AGB stars in the SMC, LMC, and Milky Way suggests that the dust-to-gas ratios in the outflows of obscured AGB stars depend approximately linearly on the initial metallicity. This was suspected by Habing et al. (1994) but still awaited observational support. The total (gas+dust) mass-loss rates of obscured AGB stars show a much weaker dependence on initial metallicity. No appreciable differences are found between these relations for obscured M-type AGB stars and obscured carbon stars.

Appendix A: new near-IR counterparts of IRAS sources in the LMC

Periods of weather conditions that were too poor for long-term photometric monitoring at the South African Astronomical Observatory (SAAO) at Sutherland, South Africa, in December 1997 were used to search for near-IR counterparts of IRAS point sources in the direction of the LMC. This was done on the 1.9 m telescope with the Mk III scanning photometer in the K-band. An aperture of $12''$ was used, chopping and nodding with a throw of $30''$. The search was limited to objects brighter than $K = 13$ mag. The areas around five IRAS point sources suspected to be obscured AGB stars (paper I) were searched. The candidate near-IR counterparts found are listed in Table A1, where the photometry is in the SAAO system (Carter 1990), i.e. the J-band magnitude is transformed to the 0.75 m telescope system. One object was re-observed under good photometric conditions (LI-LMC1284), together with the star HR2015 (δ Dor) for photometric calibration. Positions have been estimated by comparing the position of the diaphragm in the (red) acquisition video images with the second generation Digital Sky Survey, and are accurate to $\sim 2''$.

I retrieved 12, 25 and 60 μm data from the IRAS data base server in Groningen[1] (Assendorp et al. 1995). Point sources were recovered by means of 2×2 square degree maps with $0.5'$ pixels. The flux

---

[1] The IRAS data base server of the Space Research Organisation of the Netherlands (SRON) and the Dutch Expertise Centre for As-

Table A.1. Near-IR stars near IRAS point sources in the direction of the LMC (LI=LI-LMC: Schwering & Israel 1990) that are candidate obscured AGB stars. Listed are IRAS flux densities (in Jy), near-IR position, distance to the IRAS source (in arcsec), near-IR magnitudes, and bolometric magnitude assuming association (see text). Values between parentheses are 1-σ errors.

LI	F_{12}	F_{25}	F_{60}	$\alpha(2000)$	$\delta(2000)$	Δ	$J \pm \sigma_J$	$H \pm \sigma_H$	$K \pm \sigma_K$	$L \pm \sigma_L$	M_{bol}
203	0.31	0.20		4 55 40.6	$-69\,26\,40$	8	11.955(0.017)		11.858(0.039)		-5.8
				4 55 41.7	$-69\,26\,22$	26	8.776(0.016)		7.719(0.021)		-8.3
				4 55 35.7	$-69\,26\,56$	22	8.455(0.017)		7.346(0.022)	6.850(0.073)	-8.6
987	0.48	0.43		5 24 41.7	$-69\,15\,20$	15	13.006(0.069)	11.906(0.035)	11.622(0.053)		-5.7
1284	0.37	0.79		5 32 38.9	$-68\,25\,22$	13		14.015(0.049)	11.896(0.023)	9.127(0.071)	-5.8
1522	1.00	0.92		5 40 13.1	$-69\,22\,50$	3	10.660(0.015)	9.919(0.018)	8.612(0.017)	6.886(0.032)	-7.4
1795	0.25	0.28	0.16	5 56 42.7	$-67\,53\,21$	29	12.058(0.025)	11.157(0.019)	10.907(0.024)	10.336(0.129)	-5.7

density was measured from a trace through the position of the source using the command SCANAID in the Groningen GIPSY data analysis software. LI-LMC203 shows a hint of duplicity: two similarly bright sources separated by one arcminute. LI-LMC987 looks slightly extended, and LI-LMC1284 is on top of brighter emission. LI-LMC1522 and especially LI-LMC1795 are isolated. Assuming identification of near-IR and IRAS sources, the spectral energy distribution were integrated graphically to yield bolometric magnitudes.

LI-LMC203 is not identified with certainty. The best spatial coincidence is for the first listed in Table A1, that has blue near-IR colours incompatible with mass-losing AGB stars. There are two much brighter near-IR sources with moderately red $(J-K)$ nearby, of which the third listed in Table A1 is a cluster of ~ 10 stars within a diameter of $\sim 12''$. The proposed near-IR counterparts of LI-LMC987 and 1795 have near-IR colours consistent with red giants without mass loss and are probably not associated with the IRAS sources. The near-IR counterpart of LI-LMC1284 is a heavily obscured AGB star, with IR colours compatible with either carbon or oxygen-rich dust. LI-LMC1522 is also identified as a dust-enshrouded star, with IR colours suggesting oxygen-rich dust.

Appendix B: expansion velocities

Here the expansion velocities of AGB stars are briefly discussed in order to arrive at a justified calibration of the $v_{exp}(L)$ scaling relation (Eq. (3)) for LMC stars. I consider v_{exp} derived from the separation of the peaks of OH maser line profiles, and from the width of CO(1–0) emission for Milky Way stars without OH measurements. The latter are divided by 1.12, following Groenewegen et al. (1998; see also Lewis 1991).

The v_{exp} is plotted against P in Fig. B1. Periods for the LMC stars are from Wood et al. (1992) and Wood (1998), and their v_{exp} are from Wood et al. (1992) and van Loon et al. (1998b). Carbon stars (filled symbols) are distinguished from oxygen-rich, M-type stars (open symbols). As an AGB star evolves, P increases. Mass loss becomes important for $P \gtrsim 400$ d and reaches a maximum for $P \gtrsim 600$ d (cf. Jura 1986). This evolution is also reflected in v_{exp}, which increases when $P \gtrsim 400$ d and levels off at a value $v_{exp} \sim 18$ km s^{-1} for $P \gtrsim 600$ d (dotted line in Fig. B1, see also Lewis 1991). The individual data sets (and Lewis 1991) suggest that AGB stars with $P \lesssim 350$ d evolve at $\sim$constant v_{exp} typically 3 to 4 km s^{-1}. This is also seen in (intrinsic) S-type stars with semi-regular variability (Fig. 18 in Jorissen & Knapp 1998). This may be a slow wind supported by another mechanism, such

as radiation pressure on molecules (cf. Sahai & Liechti 1995; Steffen et al. 1997, 1998). It agrees with the observation that SiO masers, that depend on shocks by stellar pulsation (Alcolea et al. 1990), may be present for $P \gtrsim 350$ d and become ubiquitous when $P \gtrsim 700$ d (Izumiura et al. 1994).

Carbon stars appear to have somewhat larger v_{exp} than M-type stars at the same P, although the (few) SGC carbon stars do not obey this trend. The data is also consistent with smaller P for carbon stars at the same v_{exp}.

SGC stars within 1 kpc from the galactic plane (squares) are distinguished from SGC stars beyond that (large circles). The latter are presumably of sub-solar initial metallicity and have smaller v_{exp} than the former.

Wood et al. (1992) showed that v_{exp} is smaller at LMC metallicity than at solar metallicity, providing supportive evidence for Eq. (3). The LMC star with $v_{exp} = 24$ km s^{-1} is IRAS04553$-$6825, a very luminous RSG (van Loon et al. 1998b, and references therein). The other LMC stars are AGB stars with $v_{exp} \sim 10$ km s^{-1}. The OH/IR stars in the Groenewegen sample with $P \gtrsim 1000$ have $v_{exp} \sim 10$ to 20 km s^{-1}, suggesting that initial metallicities of these Milky Way stars are higher than the LMC stars. The expansion velocities of the obscured AGB stars in the Galactic Centre range up to $v_{exp} = 25$ km s^{-1}, and initial metallicities of two to three times solar have been suggested by Wood et al. (1998). Considering all this, Eq. (3) is calibrated by demanding a star with LMC metallicity and $L = 30,000$ L$_\odot$ ($M_{bol} = -6.5$ mag) to have $v_{exp} = 10$ km s^{-1}.

References

Alcolea J., Bujarrabal V., Gómez-González J., 1990, A&A 231, 431
Assendorp R., Bontekoe T.R., de Jonge A.R.W., et al., 1995, A&AS 110, 395
Bedding T.R., Zijlstra A.A., 1998, ApJ 506, L47
Bica E., Geisler D., Dottori H., et al., 1998, AJ 116, 723
Blommaert J.A.D.L., van der Veen W.E.C.J., van Langevelde H.J., Habing H.J., Sjouwerman L.O., 1998, A&A 329, 991
Bouchet P., Lequeux J., Maurice E., Prévot L., Prévot-Burnichon M.-L., 1985, A&A 149, 330
Carter B.S., 1990, MNRAS 242, 1
Clayton G.C., Martin P.G., 1985, ApJ 288, 558
Da Costa G.S., Hatzidimitriou D., 1998, AJ 115, 1934
de Freitas Pacheco J.A., Barbuy B., Idiart T., 1998, A&A 332, 19
Gail H.-P., Sedlmayr E., 1986, A&A 161, 201
Groenewegen M.A.T., Blommaert J.A.D.L., 1998, A&A 332, 25
Groenewegen M.A.T., Whitelock P.A., Smith C.H., Kerschbaum F., 1998, MNRAS 293, 18
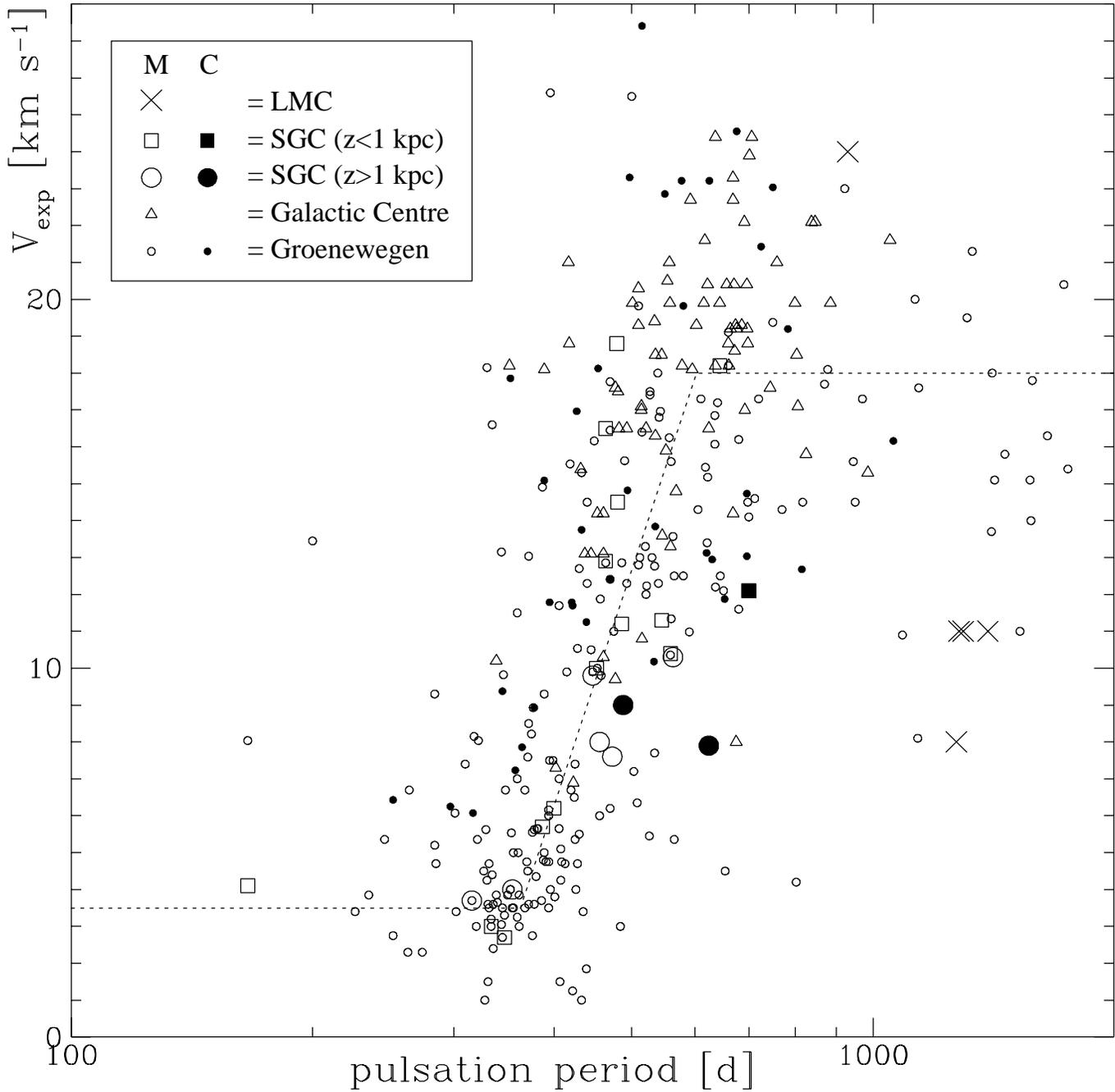Habing H.J., Tignon J., Tielens A.G.G.M., 1994, A&A 286, 523

Fig. B.1. Expansion velocity versus pulsation period, for samples in the LMC (Wood et al. 1992; Wood 1998; van Loon et al. 1998b), South Galactic Cap (Whitelock et al. 1994), Galactic Centre (Wood et al. 1998) and "Solar neighbourhood" (Groenewegen et al. 1998). Carbon stars are represented by filled symbols. The dotted line is drawn to guide the eye: expansion velocities are low for $P \lesssim 350$, increase for longer periods, and reach a more constant level for $P \gtrsim 600$. Low-metallicity stars in the LMC and SGC samples (at more than 1 kpc from the galactic plane) have lower v_{exp} than stars with $\gtrsim$ solar metallicity.

Iben I., 1981, ApJ 246, 278

Iben I., Renzini A., 1983, ARA&A 21, 271

Izumiura H., Deguchi S., Hashimoto O., et al., 1994, ApJ 437, 419

Jorissen A., Knapp G.R., 1998, A&AS 129, 363

Jura M., 1986, ApJ 303, 327

Koornneef J., 1982, A&A 107, 247

Lamers H.J.G.L.M., Cassinelli J.P., 1999, in: Introduction to Stellar Winds. Cambridge University Press, ch. 7

Lequeux J., Maurice E., Prévot-Burnichon M.-L., et al., 1982, A&A 113, L15

Lewis B.M., 1991, 101, 254

Loup C., Zijlstra A.A., Waters L.B.F.M., Groenewegen M.A.T., 1997, A&AS 125, 419 (paper I)

Loup C., Josselin E., Cioni M.-R., et al., 1999, in: Asymptotic Giant Branch Stars (IAU Symposium no. 191), eds. C. Waelkens, T. Lebertre, A. Lèbre. ASP Conf. Ser., p561

Luck R.E., Moffett T.J., Barnes T.G., Gieren W.P., 1998, AJ 115, 605

Marigo P., Girardi L., Bressan A., 1999, A&A 344, 123

Meliani M.T., Barbuy B., Richtler T., 1995, A&A 304, 347

Rich R.M., 1988, AJ 95, 828

Russell S.C., Bessell M.S., 1989, ApJS 70, 865

Sahai R., Liechti S., 1995, A&A 293, 198

Schwering P.B.W., Israel F.P., 1990, A catalog of IRAS sources in the Magellanic Clouds. Kluwer, Dordrecht

Spite F., Spite M., François P., 1989a, A&A 210, 25

Spite M., Spite F., Barbuy B., 1989b, A&A 222, 35

Steffen M., Szczerba R., Men'shchikov A., Schönberner D., 1997, A&AS 126, 39

Steffen M., Szczerba R., Schönberner D., 1998, A&A 337, 149

van den Bergh S., 1968, J. R. Astron. Soc. Can. 62, 145 & 178

van Genderen A.M., 1970, A&A 7, 49

van Loon J.Th., Zijlstra A.A., Whitelock P.A., et al., 1997, A&A 325, 585 (paper III)

van Loon J.Th., Zijlstra A.A., Whitelock P.A., et al., 1998a, A&A 329, 169 (paper IV)

van Loon J.Th., te Lintel Hekkert P., Bujarrabal V., Zijlstra A.A., Nyman L.-Å., 1998b, A&A 337, 141

van Loon J.Th., Zijlstra A.A., Groenewegen M.A.T., 1999a, A&A 346, 805

van Loon J.Th., Groenewegen M.A.T., de Koter A., et al., 1999b, A&A 351, 559

Walker A.R., 1999, in: Post Hipparcos Cosmic Candles, eds. A. Heck, F. Caputo. Astrophysics and Space Science Library vol. 237, Kluwer, Dordrecht, p125

Whitelock P.A., Menzies J.W., Feast M.W., et al., 1994, MNRAS 267, 711

Wood P.R., 1998, A&A 338, 592

Wood P.R., 1999, in: Asymptotic Giant Branch Stars (IAU Symposium no. 191), eds. C. Waelkens, T. Lebertre, A. Lèbre. ASP Conf. Ser., p151

Wood P.R., Bessell M.S., Fox M.W., 1983, ApJ 272, 99

Wood P.R., Whiteoak J.B., Hughes S.M.G., et al., 1992, ApJ 397, 552

Wood P.R., Habing H.J., McGregor P.J., 1998, A&A 336, 925

Zijlstra A.A., Loup C., Waters L.B.F.M., et al., 1996, MNRAS 279, 32 (paper II)